Am J Cancer Res 2023;13(3):818-834
www.ajcr.us /ISSN:2156-6976/ajcr0148644

Original Article

DARS2 is a prognostic biomarker and correlated with immune infiltrates and cuproptosis in lung adenocarcinoma

Xu-Sheng Liu[1*], Jing Zeng[2*], Yao-Hua Zhang[1*], Yu Zhang[1*], Yan Gao[1], Chao Liu[3], Zhi-Jun Pei[1,4]

[1]Department of Nuclear Medicine, Taihe Hospital, Hubei University of Medicine, Shiyan, Hubei, China; [2]Department of Infection Control, Taihe Hospital, Hubei University of Medicine, Shiyan, Hubei, China; [3]Medical Imaging Center, Taihe Hospital, Hubei University of Medicine, Shiyan, Hubei, China; [4]Hubei Clinical Research Center for Precise Diagnosis and Treatment of Liver Cancer, Taihe Hospital, Hubei University of Medicine, Shiyan, Hubei, China. [*]Equal contributors.

Received December 19, 2022; Accepted February 24, 2023; Epub March 15, 2023; Published March 30, 2023

Abstract: Overexpression of DARS2 may enhance the progression of hepatocellular carcinoma (HCC). However, there are few extensive reports on DARS2 function in lung adenocarcinoma (LUAD). The differential expression of DARS2 was detected by genomics and in vitro experiments, and the effect of DARS2 expression on LUAD cell activity was analyzed. Functional enrichment analysis was performed to explore possible signal pathways involved in the biological functions of DARS2 and its co-expressed genes. Utilizing TIMER and GEPIA datasets, the association between DARS2 expression and immunological infiltrating cells was analyzed. At the same time, the association between DARS2 expression pattern and LUAD m6A modification and cuproptosis was examined utilizing TCGA and GEO datasets. The level of DARS2 in LUAD increased, and inhibition of DARS2 expression could significantly inhibit the proliferation of LUAD cells. ROC curves showed that DARS2 overexpression could accurately diagnose LUAD and lead to a significant decline in the survival rates of OS, DSS, and PFI in LUAD. Enrichment analysis showed that DARS2 and its co-expressed genes were closely associated with chromosome segregation and the cell cycle. TIMER and GEPIA database analysis demonstrated that the DARS2 expression pattern was adversely correlated with the infiltration of B cells and Tfh cells. TCGA and GEO dataset examination revealed that DARS2 expression was significantly linked to four m6A-related genes and one cuproptosis-related gene. DARS2 expression is increased in LUAD patients and is closely associated with LUAD immune cell infiltration, modification of m6A, and cuproptosis. DARS2 is a potential reliable prognostic biomarker of LUAD.

Keywords: DARS2, lung adenocarcinoma, immune infiltration, m6A modification, cuproptosis

Introduction

Lung cancer is one of the most prevalent malignancies and the main cause of cancer-related deaths globally [1, 2]. With the aging of the global population, lung cancer seriously impacts global health. Lung adenocarcinoma (LUAD) is the leading form of lung cancer, which has attracted intensive research attention [2, 3]. However, despite the significant improvement in LUAD diagnosis and medication, the 5-year survival rate of LUAD is still relatively low [3, 4]. Although many scholars have done much research on LUAD, our understanding of LUAD is still very limited. Therefore, further exploring the molecular mechanism of LUAD and identifying suitable biomarkers are key scientific issues to be solved in lung cancer research.

Aspartyl-TRNA Synthetase 2, Mitochondrial (DARS2) gene encodes a mitochondrial tRNA synthetase, which accounts for the initial stage of mitochondrial protein production by enabling amino acid connection to their cognate tRNAs to ensure the correct translation of genetic codes. Previous studies have shown that the DARS2 gene has a close relationship with the development of hepatocellular carcinoma (HCC) by inhibiting apoptosis and accelerating the cell cycle. Other researchers found that DARS2 can predict the overall survival (OS) rate of LUAD and bladder urothelial carcinoma (BLCA) and

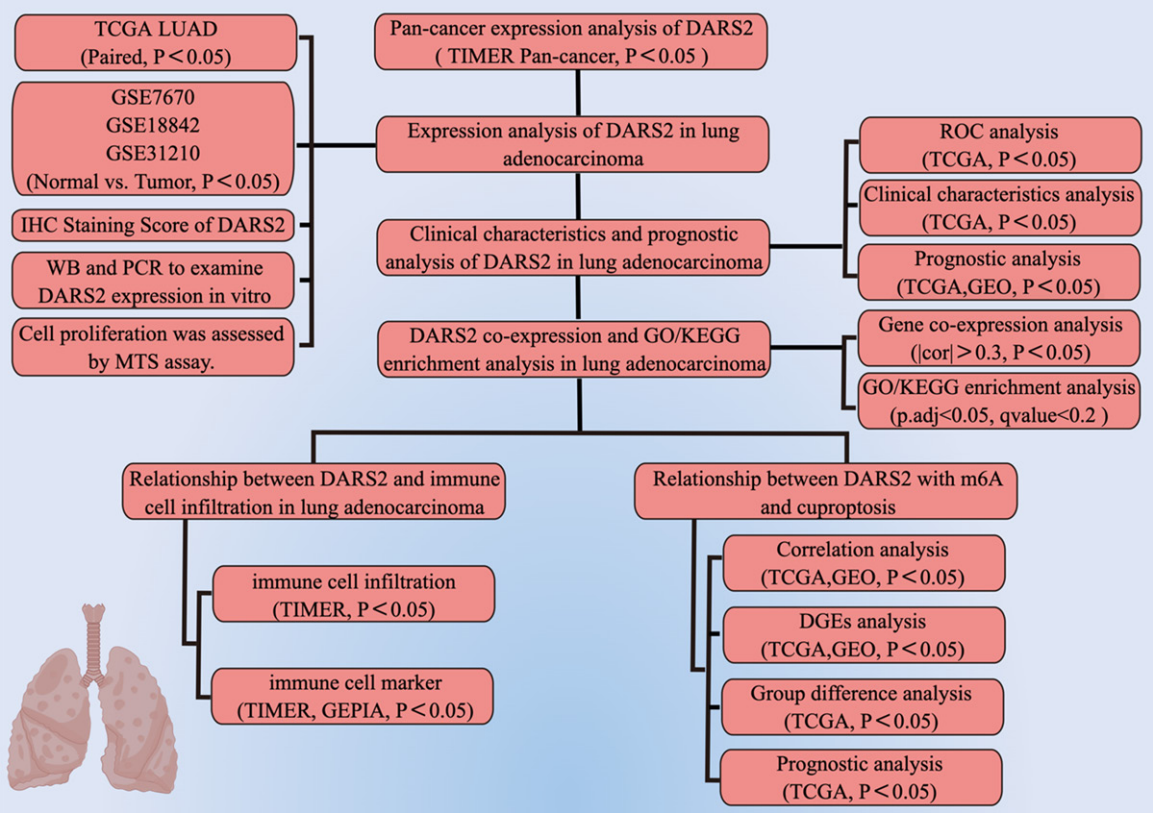

Figure 1. Flow chart of the research design. The figure was created by Figdraw (www.figdraw.com).

can be employed as a predictive model to evaluate the clinical consequences. Although some researchers have found that knocking down the expression of DARS2 can inhibit the proliferation of LUAD [5, 6], there are few extensive reports on the function of DARS2 in LUAD.

Currently, tumor microenvironment (TME), N6-methyladenosine (m6A) methylation modification and cuproptosis are the focus of targeted therapy for LUAD. Some studies have shown that LUAD cells can inhibit immune cell infiltration into the TME by using the immune system regulation mechanism to avoid antitumor immunity [7, 8]. The modification of m6A RNA is a continuous and reversible process, and m6A has been implicated in developing numerous human diseases, including tumorigenesis [9, 10]. Apoptosis, pyroptosis, and ferroptosis are all known death mechanisms; however, copper-dependent cuproptosis differs [11, 12]. Several studies have shown that unbalanced copper homeostasis interferes with apoptosis, autophagy, oxidative response, and angiogenesis, affecting tumorigenesis [13, 14]. Therefore, we would like to know whether DARS2 is associated with immunological infiltration, m6A modification, and cuproptosis regulation in LUAD, if it is implicated in carcinogenesis, and if it can be used as a potential target for anticancer therapeutics.

This research aimed to use the bioinformatics analyses and in vitro experiment to study the expression difference of DARS2 in LUAD and the correlation between DARS2, clinicopathology, and prognosis. In addition, to further exploring the molecular mechanism that DARS2 may participate in and the correlation between its expression level and immunological cell infiltration, m6A modification, and cuproptosis, which may provide better management for LUAD patients. The research roadmap is shown in **Figure 1**.

Material and methods

Expression of DARS2 in LUAD

DARS2 expression patterns in multiple cancers were evaluated using the Tumor Immune Estimation Resource (TIMER, http://timer.cis-

Table 1. Primer sequences for real time PCR

Target	Forward	Reverse
β-actin	TCTTCCAGCCTTCCTTCCT	AGCACTGTGTTGGCGTACAG
DARS2	AAGATGTGGTCCTACTAACTGC	TGTTTCTAGAAGGTCAGCACAT
HNRNPC	CGTGTACCTCCTCCTCCTCCTATTG	CCCGCTGTCCACTCTTAGAATTGAAG
YTHDF1	ATGTCGGCCACCAGCGTGGACA	TCATTGTTTGTTTCGACTCTGC

trome.org/; https://cistrome.shinyapps.io/timer/) online database [15-17]. In TIMER analysis, immunity infiltration and gene expression are systematically analyzed in numerous forms of cancer. We downloaded TCGA LUAD cohort data from the TCGA portal (https://tcga-data.nci.nih.gov/tcga/) [18]. RNA-seq data were used for gene expression evaluation, while clinical sample data were used for subsequent clinical feature analysis. Consequently, we downloaded four sequencing data containing GEO LUAD or NSCLC samples (http://www.ncbi.nlm.nih.gov/geo/; GSE7670, GSE18842, GSE31210, and GSE50081) for subsequent gene expression and prognostic analysis [19].

Immunohistochemistry (IHC)

LUAD samples and matched normal samples were obtained from 42 patients treated surgically at Taihe Hospital Affiliated of Hubei University of Medicine between 2018 and 2019. In short, tissue sections were incubated overnight with antibodies against DARS2 (1:200, Proteintech), then incubated with HRP secondary antibodies (1:500, Abcam), then stained with DAB, and finally counterstained with hematoxylin.

IHC staining scores of DARS2 was assessed by two experienced observers. IHC score of tumor cells was 0-3: 0, negative; 1, weak; 2, medium; 3, strong.

Cell culture and transfection

A549 (BNCC337696) and H1299 (BNCC100268) LUAD cell lines were obtained from the BeNa Culture Collection (BNCC, China). RPMI-1640 complete medium and incomplete medium were purchased from KeyGEN Biotech (KeyGEN, China). Cells were washed with PBS (KeyGEN, China) and treated with 0.25% trypsin (T1300, Solarbio, China). LUAD cells were transiently transfected with siRNA or si-NC using Lipofectamine 8000 (Beyotime, China). The following primers were used: siDARS2-1, Sense: 5'-GCCAACAGGUGAGAUUGAATT-3'; Antisense: 5'-UUCAAUCUCACCUGUUGGCTT-3'. siDARS2-2, Sense: 5'-CCACCUAUGGAACUGAUAATT-3'; Antisense: 5'-UUAUCAGUUCCAUAGGUGGTT-3'.

Western blot and quantitative real time PCR

The complete experimental method refers to our previous research [20]. The main experimental reagents and instruments include BCA kit (Beyotime Biotechnology), PVDF membranes (Millipore, USA), anti-DARS2 (Proteintech, China), anti-GAPDH (Cell Signaling Technology, USA), TRIzol reagent (Thermo Fisher Scientific, USA), RT Master Mix kit (TaKara, China), TB Green Premix Ex Taq Kit (TaKaRa, China), and Applied Biosystems ViiA TM 7 Real-time PCR system (Life Technologies, CA). We used β-actin as an internal control for normalization. The primer sequence used is shown in **Table 1**.

Cell viability analysis using MTS

siRNA-transfected LUAD cells were seeded into 96-well culture plates. Cell viability was measured using MTS (CellTiter 96 Aqueous One Solution Cell Proliferation Assay, Promega) assay 0, 24, 48 and 72 hours after transfection. The optical density (OD) was measured at 490 nm by the microplate reader (SpectraMax M3).

Correlation analyses between DARS2 expression and clinicopathological characteristics and prognosis

To further understand the clinical significance of DARS2, based on TCGA normal lung tissue and LUAD samples, the diagnostic role of DARS2 in LUAD was assessed through ROC curve analysis. Furthermore, we investigated the TCGA LUAD cohort to examine the relationship between DARS2 expression and clinicopathological characteristics of LUAD patients, including gender, age, pathological stage, OS, disease-specific survival (DSS) as well as progression-free survival (PFI). Meanwhile, we assessed the prognostic value of DARS2 using

the Kaplan-Meier plotter (http://kmplot.com/analysis/index.php?p=service) and PrognoScan (http://dna00.bio.kyutech.ac.jp/PrognoScan/index.html) online website. Kaplan-Meier Plotter is a database that can be accessed online and contains gene expression patterns as well as information about cancer patients' survival [21]. PrognoScan is a microarray dataset documenting the biological connection between gene expression and clinical prognosis in several malignancies [22].

Co-expression and functional enrichment analysis of DARS2 in LUAD

First, we calculated the correlation of DARS2 with other genes in the TCGA LUAD cohort using Pearson's correlation. The thresholds for co-expression were |cor| > 0.3 and P < 0.001. Then, we used heat maps to show the first 40 genes strongly and adversely linked to DARS2 expression, respectively. Simultaneously, we determined the first five genes positively linked to DARS2 expression, analyzed the correlation between these six genes, and displayed them using the circlize R package [23]. Finally, we defined a new threshold, cor > 0.05, P < 0.001, for functional enrichment testing of co-expressed genes that meet the threshold conditions by the clusterProfiler R package [24]. The functional enrichment testing includes Gene Ontology (GO; http://www.geneontology.org/) and Kyoto Encyclopedia of Genes and Genomes (KEGG; http://www.genome.ad.jp/kegg). Other findings visualizations were plotted by ggplot2 R package.

Correlation between immune infiltration and DARS2 expression patterns in LUAD

Furthermore, to investigate the possible immune regulatory mechanism of DARS2 in LUAD, the association between DARS2 expression and six immunological cells in LUAD was evaluated utilizing the TIMER database. The six immunological cells were B Cell, CD8+ T Cell, CD4+ T Cell, Macrophage, Neutrophil and Dendritic Cell. Moreover, TIMER and GEPIA were employed to investigate the association that exists in LUAD between DARS2 and immunological cell genetic markers. Previous research is referred to as immunological cell markers [9].

Correlation between m6A-related genes and DARS2 expression profiles in LUAD

Analyses of the connection between DARS2 and m6A-related gene expression patterns in the GSE50081, GSE31210, as well as TCGA LUAD cohorts were conducted using the R program. The selection of m6A-related genes refers to previous studies [25]. There are 20 genes, including ALKBH5, FTO, HNRNPA2B1, HNRNPC, IGF2BP1, IGF2BP2, IGF2BP3, METTL14, METTL3, RBM15, RBM15B, RBMX, VIRMA, WTAP, YTHDC1, YTHDC2, YTHDF1, YTHDF2, YTHDF3, and ZC3H13. Employing the limma R tool, we assessed the expression differences of the above-mentioned m6A-associated genes in the GSE31210 and TCGA LUAD cohorts. In the TCGA LUAD cohort, the level of DARS2 expression was classified into two different (high and low) expression categories. The levels of expression of m6A-related genes were then examined between the two groups. Therefore, the prognosis of genes correlated with m6A found in the TCGA LUAD cohort was evaluated. Finally, the UpSetR R program was used to screen and display the positive genes that meet the above requirements. Other data visualizations were plotted by ggplot2 R package. In order to further verify the potential relationship between DARS2 and m6A, we detected the expression level of HNRNPC and YTHDF1 in H1299 cell line after interfering with DARS2 expression.

Correlation between cuproptosis-related genes and DARS2 expression in LUAD

The R program assessed the connection between DARS2 expression and cuproptosis gene expression in the GSE50081, GSE31210, and TCGA LUAD cohorts. The choice of cuproptosis-related genes corresponds to earlier studies [11]. There are 10 genes, FDX1, LIAS, LIPT1, DLD, DLAT, PDHA1, PDHB, MTF1, GLS and CDKN2A. Concurrently, we investigated the gene expression variations of the cuproptosis mentioned above genes in the GSE31210 and TCGA LUAD cohort by employing the limma R tool. In the TCGA LUAD cohort, DARS2 expression was categorized into high and low expression categories. Variations in cuproptosis-related gene expression in the two expression groups were further investigated. Additionally, the prognosis of cuproptosis-related genes was examined in the TCGA LUAD cohort. Finally, the UpSetR R program was used to detect and dis-

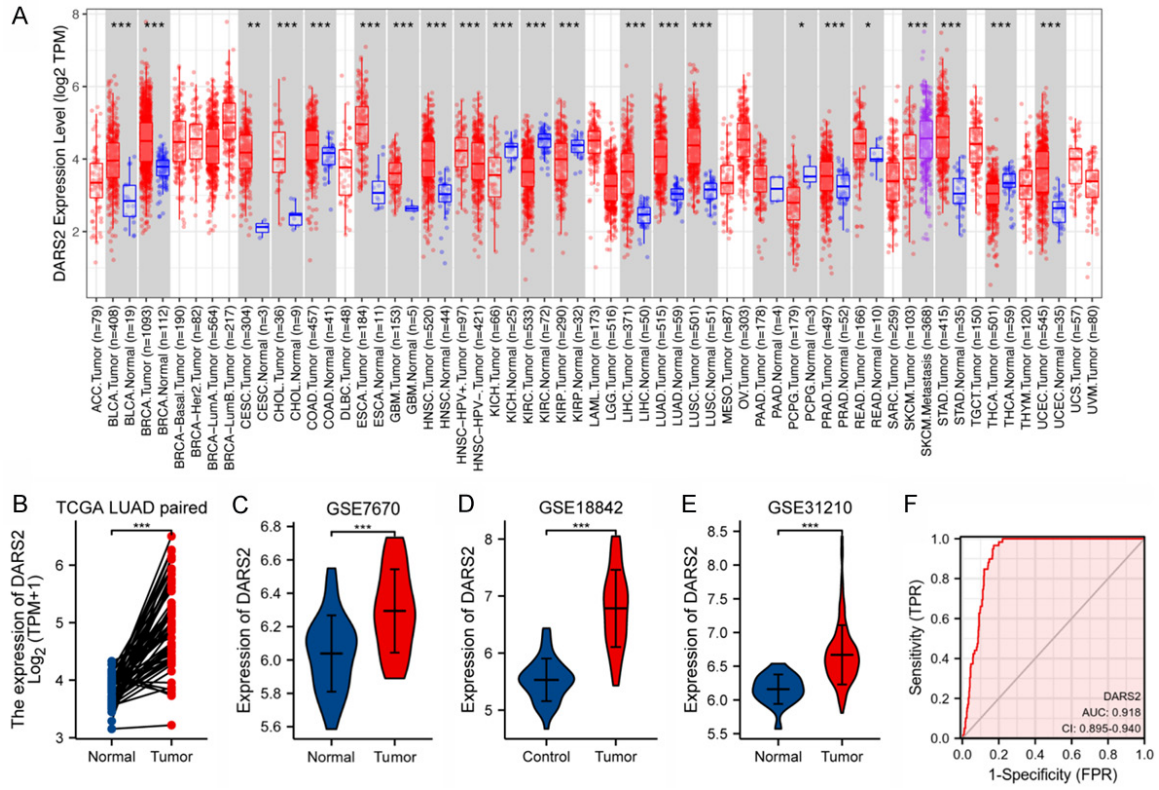

Figure 2. DARS2 expression in LUAD. A. The TIMER data analyzed the expression difference of DARS2 in pan-cancer; B. The expression difference of DARS2 in TCGA LUAD paired samples; C-E. Expression differences of DARS2 between tumorous samples and control samples in GSE7670, GSE11842 and GSE31210 datasets; F. ROC curve demonstrating the diagnostic value of DARS2 expression based on TCGA LUAD cohort. *, P < 0.05; **, P < 0.01; ***, P < 0.001.

play positive genes that meet the above requirements. Other data visualizations were plotted using the ggplot2 R package.

Statistical methods

Most statistical analysis is done through the bioinformatics mentioned above tools; this includes the Xiantao platform (www.xiantao.love), a database that integrates data from TCGA tumor chips, which contains R software and its appropriate R software package. It is primarily utilized on behalf of gene expression, correlation, enrichment, interactive network, clinical significance, and related mapping analyses. P < 0.05 was judged as statistically significant.

Results

Expression of DARS2 in LUAD

When analyzing the expression of DARS2 in several cancers, we referred to the TIMER database for our research. **Figure 2A** demonstrates that the pattern of DARS2 expression in 15 cancers was significantly elevated contrasted with the control group, including BLCA (P = 7.25E-08), breast invasive carcinoma (BRCA, P = 2.81E-26), cervical squamous cell carcinoma and endocervical adenocarcinoma (CESC, P = 3.30E-03), cholangiocarcinoma (CHOL, P = 5.98E-07), colon adenocarcinoma (COAD, P = 6.15E-04), esophageal carcinoma (ESCA, P = 3.00E-07), glioblastoma multiforme (GBM, P = 3.00E-04), head and neck squamous cell carcinoma (HNSC, P = 1.94E-16), liver hepatocellular carcinoma (LIHC, P = 3.02E-20), LUAD (P = 9.81E-27), lung squamous cell carcinoma (LUSC, P = 5.75E-27), prostate adenocarcinoma (PRAD, P = 2.90E-04), rectum adenocarcinoma (READ, P = 3.52E-02), stomach adenocarcinoma (STAD, P = 7.61E-18) and uterine corpus endometrial carcinoma (UCEC). However, the expression level of DARS2 in five tumors was significantly reduced compared to the control group, including kidney chromo-

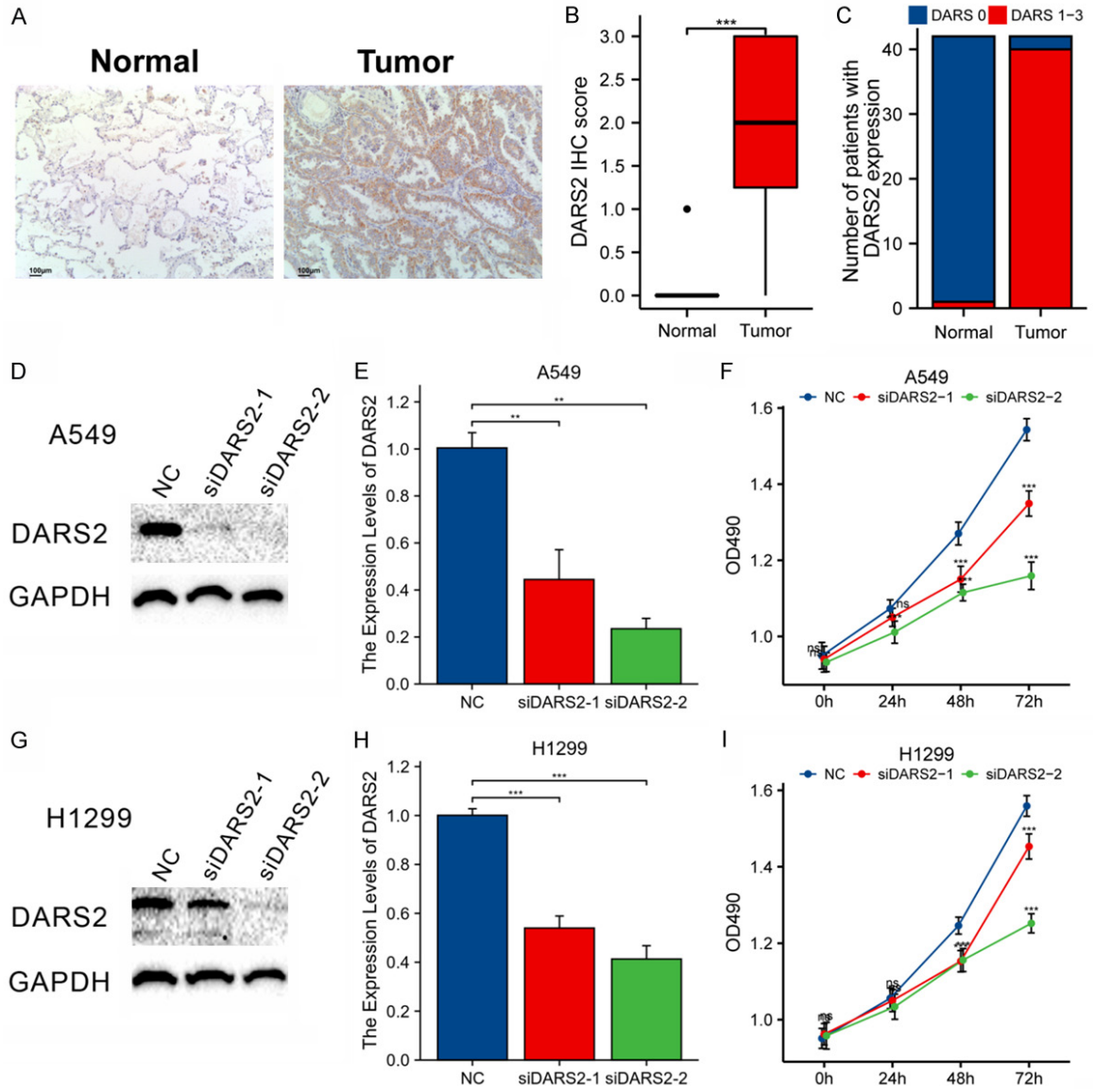

Figure 3. DARS2 knockdown inhibits cell proliferation. A. IHC staining picture of DARS2; B, C. The expression difference of DARS2 between the LUAD samples and the normal samples were analyzed using the IHC (Wilcoxon rank sum test); D, G. Western blot analysis confirming the success of siDARS2 transfection; E, H. qRT-PCR analysis confirming the success of siDARS2 transfection; F, I. Silencing of DARS2 expression reduced the growth of A549 and H1299 cells. *, P < 0.05; **, P < 0.01; ***, P < 0.001.

phobe (KICH, P = 9.72E-06), kidney clear cell carcinoma (KIRC, P = 1.59E-29), kidney renal papillary cell carcinoma (KIRP, P = 2.33E-04), pheochromocytoma and paraganglioma (PCPG, P = 2.56E-02) and thyroid carcinoma (THCA, P = 3.02E-08). See Supplementary Table 1 for the differential analysis results of Pan-cancer expression of DARS2. Therefore, we analyzed the paired data in TCGA LUAD cohort data and three GEO cohort data to confirm the expression difference of DARS2 between LUAD samples and healthy tissues. According to our findings, the expression pattern of DARS2 in the tumor group was significantly elevated, contrasted with the typical control group (**Figure 2B-E**, P < 0.001). These findings were based on data from TCGA LUAD paired samples and the GEO cohort.

DARS2 knockdown inhibits cell proliferation

IHC staining further verified the expression of DARS2 protein in LUAD and control samples (**Figure 3A**). Statistical analysis showed that

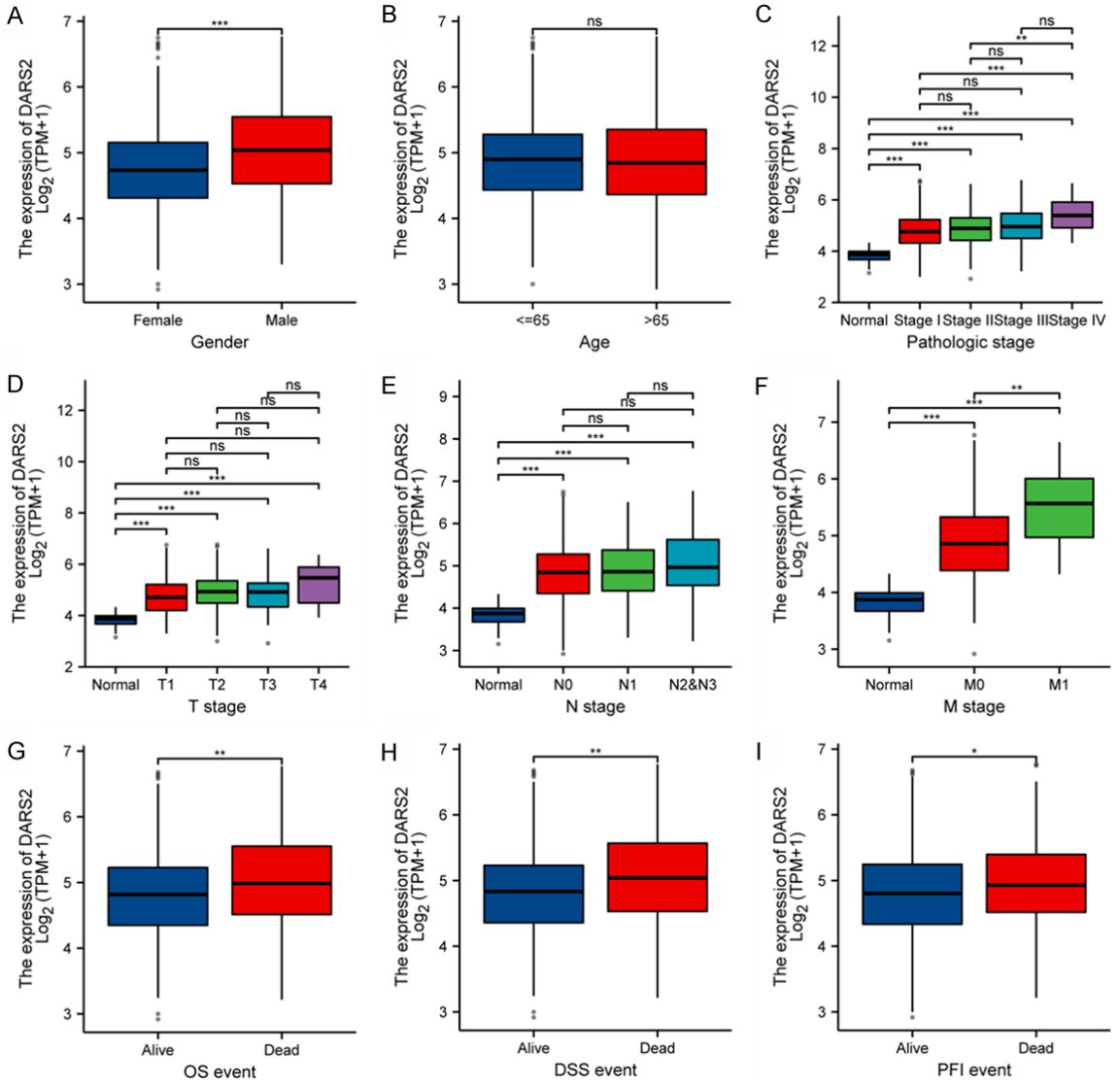

Figure 4. A-I. Correlation analyses between the expression of DARS2 and the clinicopathological characteristics. *, P < 0.05; **, P < 0.01; ***, P < 0.001.

the expression of DARS2 in LUAD was significantly higher than that in normal samples (**Figure 3B**, **3C**). In order to explore the effect of DARS2 on LUAD cells, siRNA was used to interfere with the expression of DARS2 in A549 and H1299 cells. The interference efficiency was confirmed by Western blot (**Figure 3D**, **3G**, P < 0.05) and qRT-PCR (**Figure 3E**, **3H**, P < 0.05) analysis. We used MTS assay to determine the proliferation activity of the two transfected cells. The results showed that the cell proliferation activity of the two siRNA groups was significantly lower than that of the siRNA control group (**Figure 3F**, **3I**, P < 0.05).

Correlation analyses between DARS2 expression and clinicopathological characteristics and prognosis

To further explore the diagnostic accuracy of DARS2 for LUAD, ROC curves were constructed, and the ROC area under the curve (AUC) was computed. ROC curve results demonstrated that DARS2 has a diagnostic value in LUAD (AUC: 0.918; CI: 0.895-0.940; P < 0.05) (**Figure 2F**). However, in the correlation analysis of clinical features, we observed the DARS2 expression to be significantly elevated in male patients in comparison with female patients (**Figure 4A**, P < 0.001), but DARS2 expression showed no

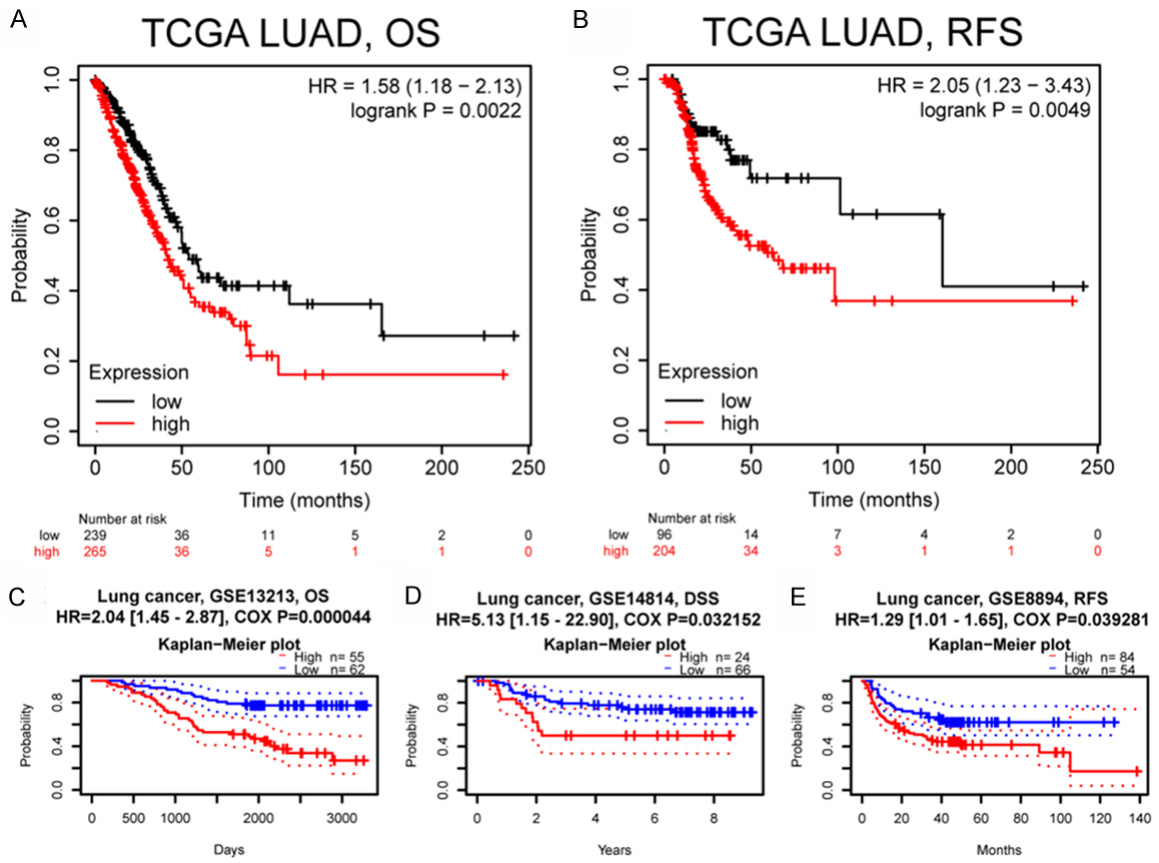

Figure 5. Correlation analyses between the expression of DARS2 and prognosis. A, B. Kaplan-Meier analysis of OS and RFS of the above patients in the TCGA LUAD cohort; C-E. Kaplan-Meier survival analysis was utilized to analyze the association between DARS2 expression and OS, DSS and RFS in LUAD patients in GEO database.

relation with age (**Figure 4B**, P > 0.05). In the pathological stage, the expression level of DARS2 in stage IV was significantly elevated compared with stage I and stage II (**Figure 4C**, P < 0.05). The findings demonstrated no significant variation in the expression of DARS2 between the pathological T stage and pathological N stage (**Figure 4D**, **4E**, P > 0.05). However, in the pathological M stage, the DARS2 expression pattern in M1 was significantly elevated in comparison with M0 (**Figure 4F**, P < 0.001). In prognostic events (OS event, DSS event and PFI event), the DARS2 expression level was significantly increased in dead subjects compared with in alive subjects (**Figure 4G-I**, P < 0.05). Meanwhile, through Kaplan-Meier plotter and PrognoScan analysis, we found that DARS2 expression level in patients is associated with poorer OS, DSS and recurrence-free survival (RFS) (**Figure 5**, P < 0.05).

Co-expression and functional enrichment analysis of DARS2 in LUAD

Pearson's correlation test found that 2978 protein-coding genes were positively correlated with DARS2 expression, and 101 protein-coding genes showed a negative correlation. Volcano map shows the distribution of co-expressed genes with correlation (**Figure 6A**). Simultaneously, we demonstrated the foremost 40 genes positively or adversely linked to DARS2 expression by heat map (**Figure 6B**, **6C**; Supplementary Table 2). According to the correlation coefficient values, we screened the top five genes, including URB2 (URB2 Ribosome Biogenesis Homolog), NDUFS1 (NADH: Ubiquinone Oxidoreductase Core Subunit S1), IARS2 (Isoleucyl-TRNA Synthetase 2, Mitochondrial), LRPPRC (Leucine Rich Pentatricopeptide Repeat Containing) and UCHL5 (Ubiquitin C-Terminal Hydrolase L5). Interestingly, we found that these six genes were significantly

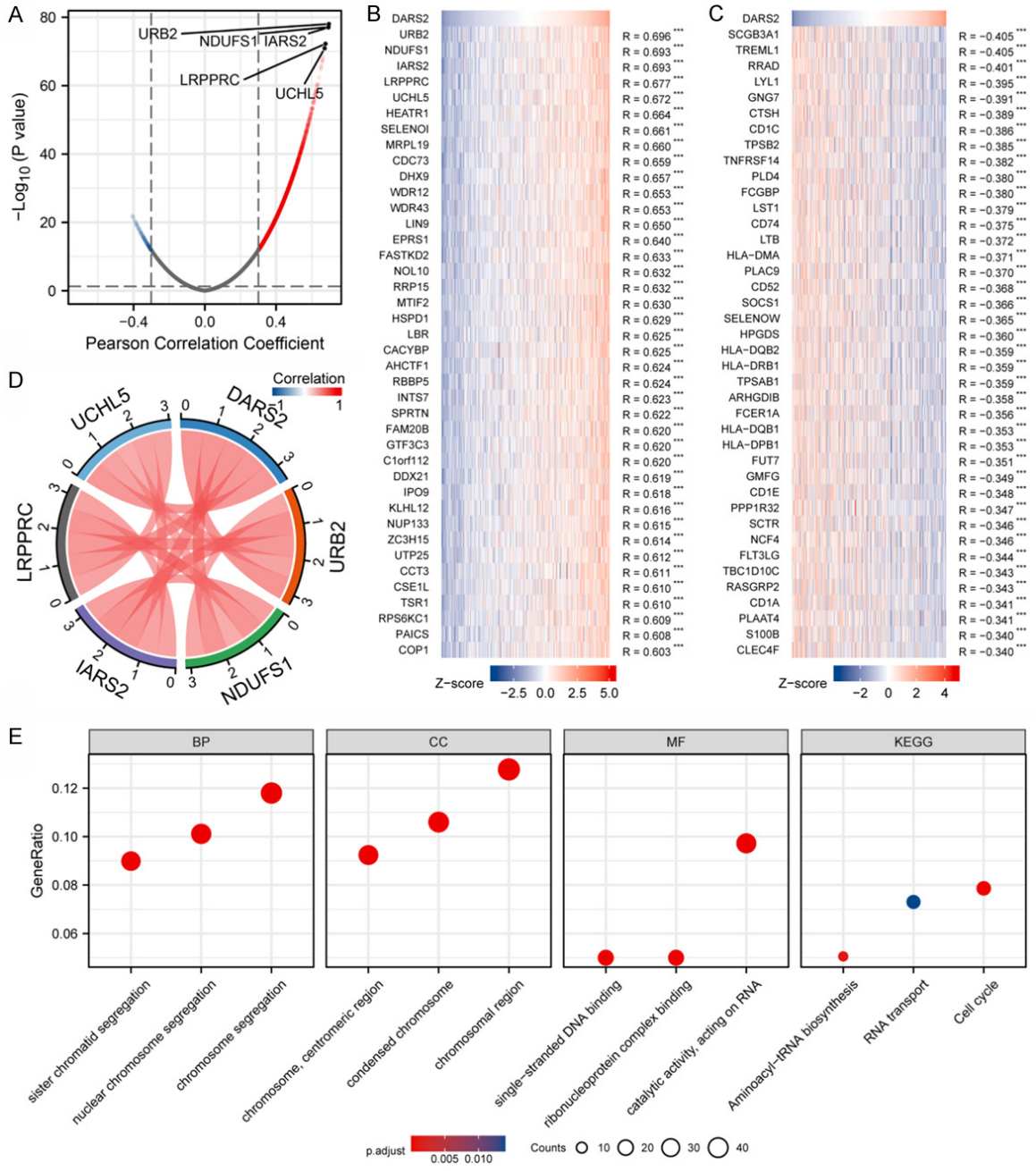

Figure 6. Co-expression and functional enrichment analysis of DARS2 in LUAD. A. Volcano map shows the distribution of co-expressed genes with correlation; B, C. Top 40 genes positively or adversely linked to DARS2 expression by heat map; D. The circled plot shows the correlation between the six genes; E. The bubble diagram shows the enrichment analysis of DARS2 and its co-expressed genes. ***, P < 0.001.

correlated with each other (**Figure 6D**, cor > 0.5, P < 0.001). To analyze the possible biological activities of DARS2 and its co-expressed genes, we redefined the threshold as cor > 0.05, P < 0.001, and finally, we got 375 co-expressed genes. Through the enrichment analysis of DARS2 and the above 375 co-expressed genes, we found that the GO enrichment analysis identified 629 enriched GO terms (445 BP, 106 MF, and 78 CC), and the KEGG enrichment analysis identified eight KEGG pathways. DARS2 and its co-expressed genes are mainly involved in the chromosome segregation, chromosomal region, cata-

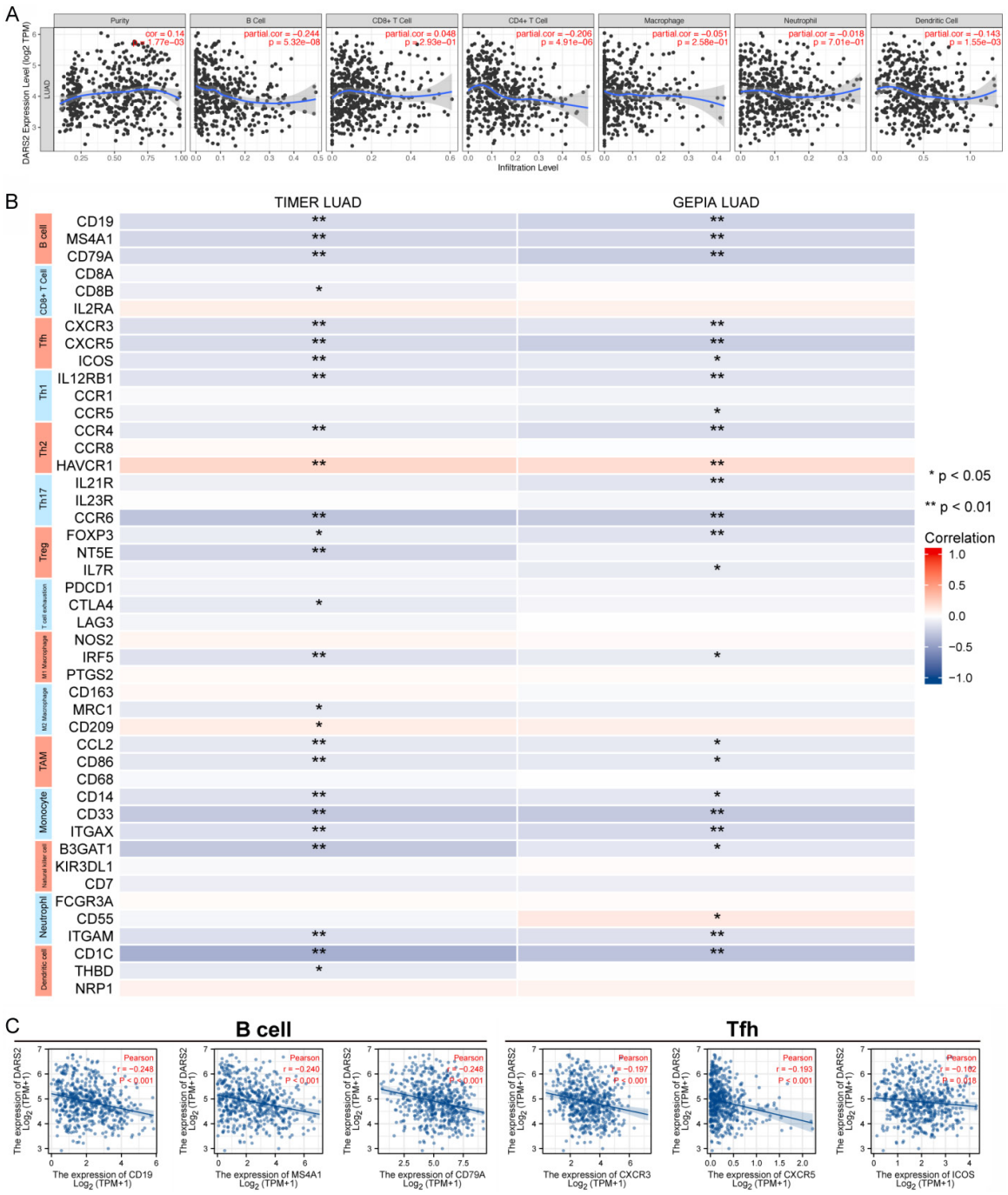

Figure 7. Correlation between immune infiltration and DARS2 expression in LUAD. A. Research on the relationship between DARS2 expression and immunological cell infiltration; B. Research of the relationship between DARS2 expression and immunological cell marker genes; C. DARS2 expression was linked to B cell and Tfh in LUAD.

lytic activity, acting on RNA and Cell cycle of LUAD (**Figure 6E**; Supplementary Table 3).

Correlation between immune infiltration and DARS2 expression in LUAD

Using timer data, we analyzed the relationship between DARS2 expression and immunological cell infiltration in LUAD. According to the findings, the level of expression of DARS2 was found to have a negative association with the expression patterns of B cells (r = -0.244, P = 5.32e-8), CD4+ T cells (r = -0.206, P = 4.91e-6) and dendritic cells (r = -0.143, P = 1.55e-3) (**Figure 7A**). Meanwhile, we analyzed the connection between DARS2 and immunity marker

genes of multiple immunological cells utilizing the TIMER and GEPIA databases (**Figure 7B**). Analysis revealed that DARS2 expression was related to B cells, Tfh, and monocyte immunity marker genes, such as CD19, MS4A1, CD79A, CXCR3, CXCR5, ICOS, CD14, CD33 and ITGAX. Combined analysis of immune cell infiltration and immune cell gene markers, we screened gene markers of B cells and Tfh and displayed them using scatter plots (**Figure 7C**).

Correlation between m6A-related genes and DARS2 expression in LUAD

In tumorigenesis, proliferation, and metastasis, m6A modification plays a crucial role. We investigated the connection between DARS2 expression and 20 m6A-related gene expression in LUAD by examining GSE50081, GSE31210 and TCGA LUAD cohort results. These results showed that DARS2 expression was significantly associated with ALKBH5, HNRNPC, IGF2BP1, IGF2BP3, RBM15, YTHDF1, as well as YTHDF3 in the cohort data of GSE50081, GSE31210 and TCGA LUAD (**Figure 8A**, $P < 0.05$). Furthermore, in GSE50081, DARS2 expression was positively linked to both IGF2BP2 and WTAP expressions and adversely linked to the expression of METTL14, YTHDC2 and ZC3H13 (**Figure 8A**, $P < 0.05$). In GSE31210, DARS2 was positively correlated with the expression of RBM15B and adversely linked to the expression of METTL14, METTL3, RBMX, WATP, YTHDC1, YTHDC2 and ZC3H13 (**Figure 8A**, $P < 0.05$). In the TCGA LUAD cohort data, DARS2 was positively linked to the expression of FTO, HNRNPA2B1, IGF2BP2, METTL14, METTL3, RBM15B, RBMX, VIRMA, WTAP, YTHDC1, YTHDC2, YTHDF2, as well as ZC3H13 (**Figure 8A**, $P < 0.05$). Through limma differential expression analysis, the findings revealed significant variations in FTO, HNRNPC, IGF2BP1, IGF2BP3, METTL14, RBM15, RBMX, WTAP, YTHDF1, YTHDF2 and ZC3H13 expression between tumor samples and control samples in GSE31210 and TCGA LUAD cohort data (**Figure 8B**, $P < 0.05$). In the difference analysis between the two DARS2 groups, we observed significant variations in these 20 genes, and the expression level of these 20 genes in the high DARS2 expression group was increased compared with the DARS2 low expression group (**Figure 8C**, $P < 0.05$). In further prognostic analysis, we observed that the expression patterns of seven genes had prognostic effects; moreover, the genes with elevated expression predicted worse OS, namely ALKBH5, HNRNPA2B1, HNRNPC, IGF2BP1, IGF2BP2, IGF2BP3 and RBM15 (**Figure 8D**, $P < 0.05$). Finally, we screened the positive genes that met the above conditions and displayed them using UpSetR R package (**Figure 8E**, $P < 0.05$). We found that simultaneously HNRNPC, IGF2BP1, IGF2BP3, and RBM15 met all the above screening conditions. Cell experiments showed that the expression of HNRNPC and YTHDF1 genes decreased significantly after interfering with the expression of DARS2 (**Figure 8F**, $P < 0.05$).

Correlation between cuproptosis-related genes and DARS2 expression in LUAD

The induction of cuproptosis is becoming a promising method to manage human cancer. We investigated the relationship between DARS2 expression and 10 cuproptosis genes expression in LUAD by examining GSE50081, GSE31210 and TCGA LUAD cohort data. These findings declared that DARS2 expression was significantly positively associated with CDKN2A, DLAT, PDHA1 and PDHB in the GSE50081, GSE31210, and TCGA LUAD cohort data (**Figure 9A**, $P < 0.05$). Furthermore, in GSE50081, DARS2 expression was adversely linked to the expression of GLS (**Figure 9A**, $P < 0.05$). In GSE31210, DARS2 was positively linked to the expression of DLD and LIAS (**Figure 9A**, $P < 0.05$). In the TCGA LUAD cohort data, DARS2 was positively linked to the expression of DLD, LIAS, LIPT1 and MTF1 (**Figure 9A**, $P < 0.05$). Limma differential expression analysis revealed significant variations in CDKN2A, DLAT, LIAS and MTF1 expression between tumorous samples and control samples in GSE31210 and TCGA LUAD cohort data (**Figure 9B**, $P < 0.05$). We observed significant variations in seven distinct genes when we compared the high DARS2 group to the low DARS2 group using different expression analyses. Compared to the DARS2 low expression group, the level of expression of these seven genes was significantly increased when they were studied in the DARS2 high expression group. The seven genes were DLAT, DLD, LIAS, LIPT1, MTF1, PDHA1, PDHB, respectively (**Figure 9C**, $P < 0.05$). In further prognostic analysis, we found that the expression levels

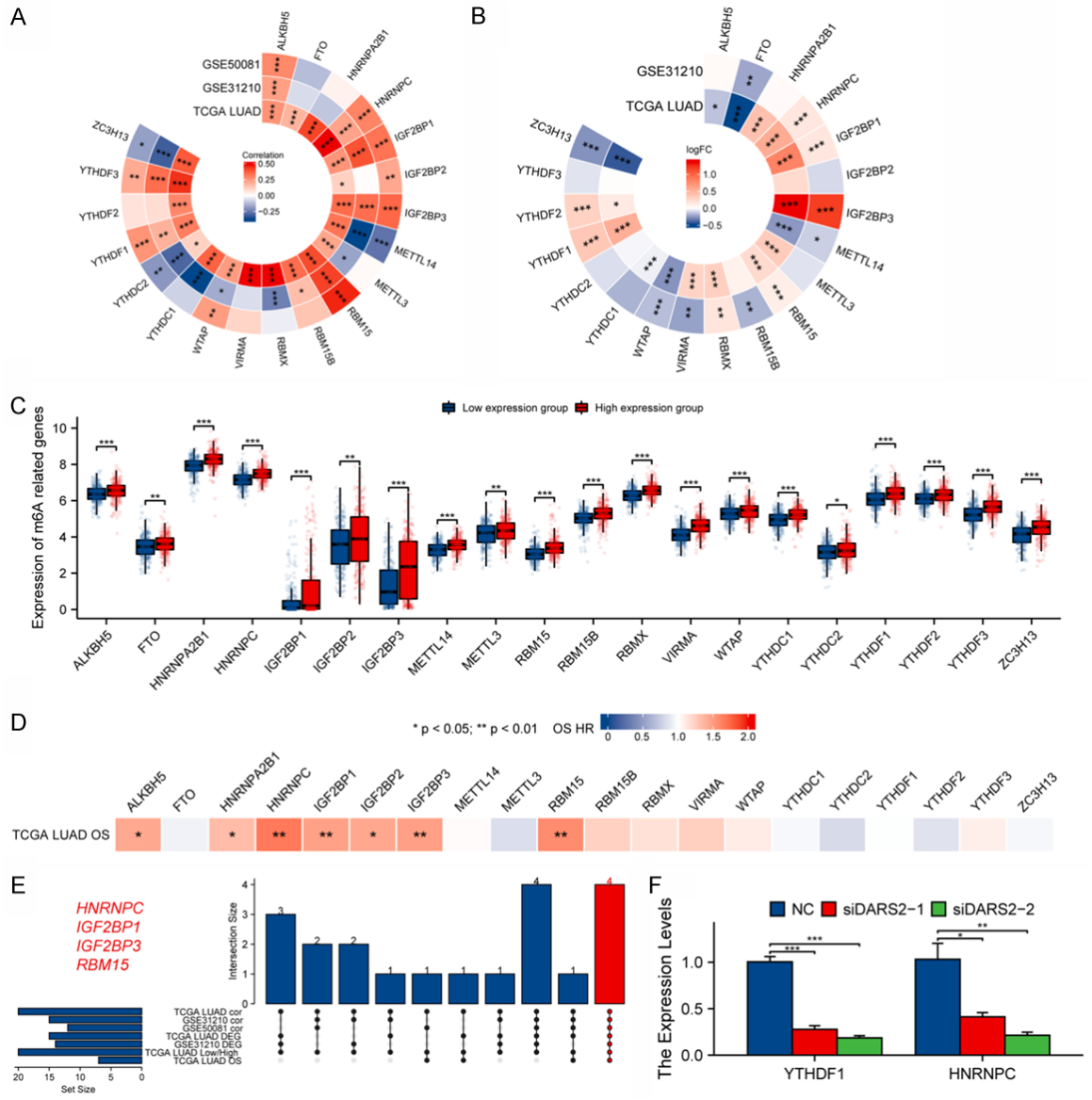

Figure 8. Correlation between m6A-related genes and DARS2 expression in LUAD. A. Relationship between DARS2 expression and m6A-related genes expression in GSE50081, GSE31210 and TCGA LUAD cohort; B. Using the limma R package, the expression differences of the m6A-related genes in the GSE31210 and TCGA LUAD cohort; C. Differential expression of m6A associated genes in the two DARS2 expression groups; D. Analyzed m6A associated genes prognosis in TCGA LUAD cohort; E. The UpSetR R package was used to screen and display the positive genes that meet the above requirements; F. Cell experiment confirmed that the expression of YTHDF1 and HNRNPC decreased after interfering with DARS2. *, P < 0.05; **, P < 0.01; ***, P < 0.001.

of DLD had prognostic effects, and the high expression of genes predicted worse OS (**Figure 9D**, **9E**, P < 0.05). Finally, we screened positive genes that met the above conditions and displayed them using the UpSetR R package. Because the results of prognosis analysis are too few, we excluded the results of prognosis analysis in UpSetR analysis (**Figure 9F**, P < 0.05). We found that DLAT met all of the above screening conditions simultaneously.

Discussion

Lung cancer has the highest incidence and mortality worldwide [1, 2]. LUAD is a common histological form of lung cancer [3]. After that, it is essential to recognize new biomarkers and pathways for treating LUAD [2]. In previous studies, DARS2 estimated the OS of LUAD [26-28] and BLCA [29-31] as a prognostic model. Jin et al. [6] and Jiang et al. [5] found that

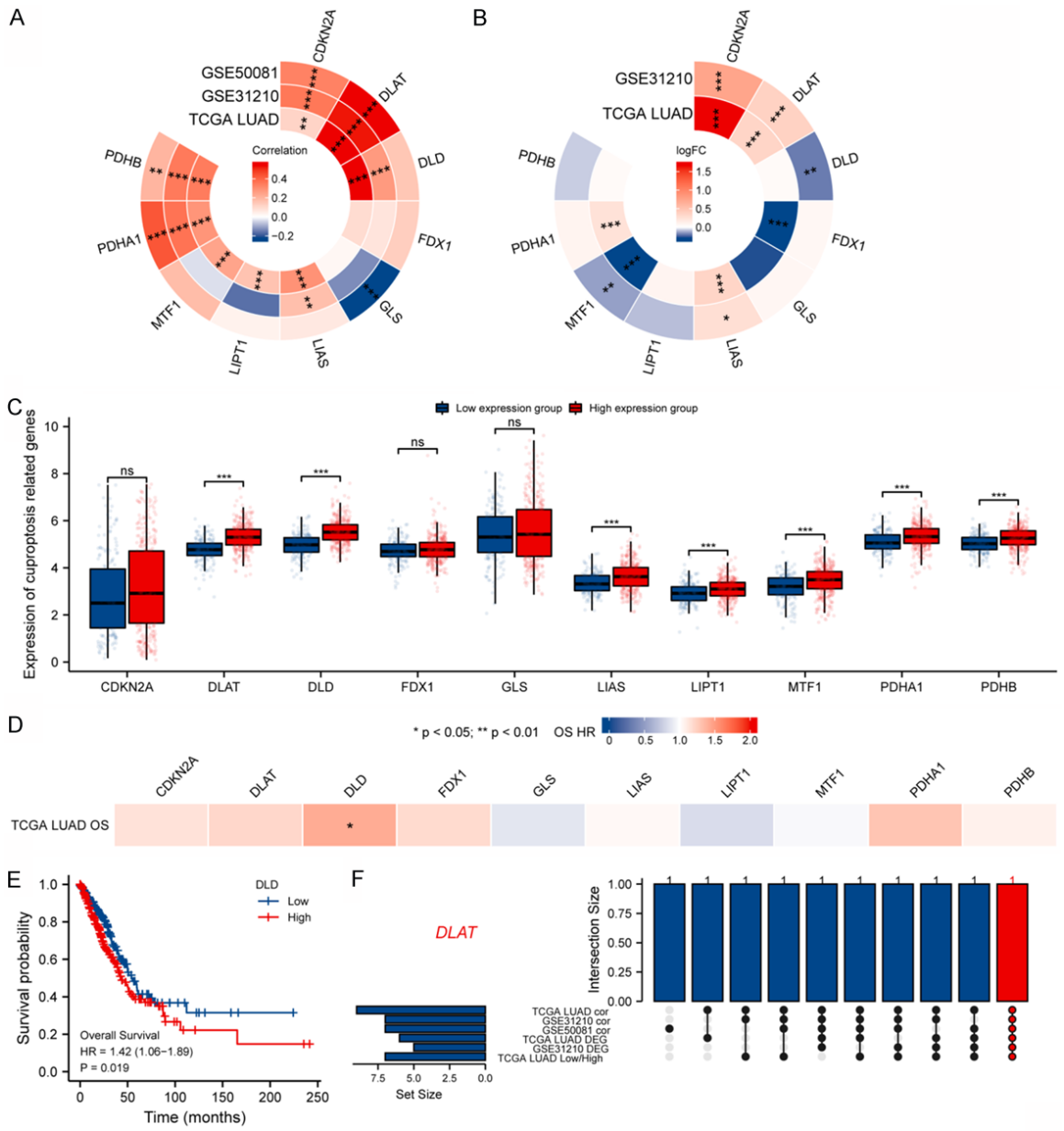

Figure 9. Correlation between cuproptosis-related genes and DARS2 expression in LUAD. A. Relationship between DARS2 expression and cuproptosis-related genes expression in GSE50081, GSE31210 and TCGA LUAD cohort; B. Using the limma R package, the expression differences of the m6A-related genes in the GSE31210 and TCGA LUAD cohort; C. Differential expression of cuproptosis-related genes in the two DARS2 expression groups; D, E. Analyzed cuproptosis-related genes prognosis in TCGA LUAD cohort; F. The UpSetR R package was used to screen and display the positive genes that meet the above requirements. *, P < 0.05; **, P < 0.01; ***, P < 0.001.

knocking down the expression of DARS2 could significantly inhibit the proliferation of LUAD. Qin et al. [32] found that DARS2 is overexpressed in HCC and can promote the progression of the HCC cell cycle and inhibit apoptosis of HCC cells, thus promoting the development of HCC. However, there is no comprehensive analysis of DARS2 in LUAD.

This investigation found that DARS2 expression increased in many cancers by analyzing TCGA and GEO data. This expression pattern is associated with the clinicopathological parameters of many patients with LUAD. We also found that highly expressed DARS2 can accurately predict LUAD outcomes. Concurrently, patients with high DARS2 expression

exhibit poorer prognoses, consistent with previous findings [26-28]. These results suggest that DARS2 may promote LUAD and may be a potential predictive and diagnostic indicator.

To understand and interpret the regulating function of DARS2 in LUAD, we conducted a co-expression analysis. Through co-expression analysis, we first screened the top five genes positively correlated with DARS2 expression, namely URB2, NDUFS1, IARS2, LRPPRC and UCHL5. Zhan et al. [33] found that NDUFS1 showed reduced expression in LUAD cells, and overexpression of NDUFS1 could inhibit the growth and migration of LUAD cells. Yin et al. [34] found that IARS2 silencing induced growth inhibition and cell cycle arrest and promoted apoptosis of NSCLC cells. Tian et al. [35] found that LRPPRC exerts a significant role in LUAD by its antiapoptotic and high invasiveness properties. According to Liu et al. [36], UCHL5 can enhance the growth and metastasis of LUAD induced by EIF3m. In the enrichment analysis of DARS2 co-expressed genes, we found that DARS2 and its co-expressed genes were mainly included in the chromosome segregation, chromosomal region, catalytic activity, acting on RNA, and the LUAD cell cycle. The above results indicate that DARS2 and its co-expressed genes play a key role in establishing LUAD, so we speculate that DARS2 can also participate in developing LUAD through different biological functions.

In view of the important role of immune regulation in LUAD, we tried to explore the relationship between DARS2 expression and immune cell infiltration in LUAD. The results showed that DARS2 was negatively correlated with immune cells (B cell and Tfh). Interestingly, this study found that the expression of DARS2 in LUAD was significantly up-regulated, and the up-regulated expression of DARS2 may reduce the infiltration level of B cell and Tfh. However, the lower level of B cell infiltration can predict a worse survival period of LUAD patients [37]. In summary, these data provide new insights into the immune mechanism of DARS2 in LUAD, which will lay the foundation for targeted prevention, progression monitoring, prognostic assessment, and personalized medicine.

Various cancers have been linked to abnormalities in the modification of m6A on RNA [38, 39]. By analyzing the TCGA and GEO datasets, we discovered four m6A-related genes, HNRNPC, IGF2BP1, IGF2BP3 and RBM15, met the expression-related genes, grouping difference genes and prognostic value genes. Yan et al. [40] found that overexpression of HNRNPC in NSCLC cell lines can significantly enhance tumor cell aggressiveness in vitro and in vivo. Huang et al. [41] discovered that circxpo1 promotes the growth and migration of LUAD through interacting with IGF2BP1 and regulating the transcriptional stability of CTNNB1. As per Yan et al. [42] findings, IGF2BP3 promoted the progression of lung cancer cells by down-regulating miR-1202. Ma et al. [43] observed that RBM15 showed elevated expression in LUAD tissues and cells, and RBM15 knockdown could reduce methylation levels, reduce proliferation, accelerate apoptosis, and inhibit tumor growth. If the prognostic value is unconsidered, YTHDF1 and DARS2 are significantly correlated, with significant differences between different groups. Shi et al. [44] observed that YTHDF1 depletion decreased NSCLC cell growth and xenograft carcinogenesis through modulating CDK2, CDK4, and cyclin D1 translation effectiveness. In summary, we believe that the promotion of DARS2 in the emergence and progression of LUAD can be associated with m6A alteration, which can influence the level of LUAD methylation by altering the expression level of HNRNPC, IGF2BP1, IGF2BP3, RBM15 and YTHDF1, and then affect the progress of LUAD. Interestingly, in vitro cell experiments confirmed that the expression level of HNRNPC and YTHDF1 genes decreased significantly after interfering with the expression of DARS2. Although bioinformatics analysis showed that the expression of YTHDF1 had no prognostic significance, YTHDF1 was significantly correlated with DARS2 in LUAD data set, and there was significant difference between tumor samples and normal samples. Therefore, we speculate that HNRNPC and YTHDF1 genes may be potential targets of DARS2, and may affect the progress of LUAD by regulating the expression of HNRNPC and YTHDF1.

Cuproptosis and copper are closely related to cancer genesis, severity, and progression, making them vulnerable targets for cancer prevention [12, 13]. A meta-analysis included 33 articles, including 3026 cases and 9439 controls.

The combined results showed that the serum copper level of lung cancer patients was increased compared with that of the healthy control group, suggesting that elevated serum copper levels can raise the risk of lung cancer [45]. This research declared that only DLAT met the conditions of expression pattern correlation and grouping difference significance simultaneously. Chen et al. found that the increased DLAT expression positively correlated with the tumor size, bad fate and SUVmax value of ^{18}F-FDG PET/CT scanning of NSCLC patients, suggesting that DLAT-related pathways may be targets of NSCLC treatment [46]. Therefore, we believe that the promotion of DARS2 on the onset and progression of LUAD may be connected with DLAT, and the overexpression of DARS2 in LUAD may affect the copper ion imbalance of LUAD by impairing DLAT expression and then affect the progress of LUAD.

Despite the fact that this contributes to the literature on the reliability of DARS2 as a prognostic biomarker of LUAD, it is important to keep in mind that it is not without its drawbacks. First, most of our study inputs were collected through online databases, so we could not assess the quality of the data. Second, further experiments are needed to validate our findings.

Conclusions

We concluded that increased DARS2 expression in LUAD patients predicts a worse survival prognosis and is closely related to aggressive clinical features, unfavourable immune infiltration, m6A modification and cuproptosis. The present results revealed that DARS2 could serve as a novel prognostic and diagnostic biomarker of LUAD. However, the DARS2 mechanism that regulates LUAD tumorigenesis and progression needs further clarification.

Acknowledgements

This work was supported by the Hubei province's Outstanding Medical Academic Leader program, the Foundation for Innovative Research Team of Hubei Provincial Department of Education T2020025, the general project of Hubei Provincial Department of Education (No. B2021160), Innovative Research Program for Graduates of Hubei University of Medicine (grant no. YC2022042, YC2022037), Shiyan Taihe Hospital hospital-level project (2022JJXM007) and the Key Discipline Project of Hubei University of Medicine.

Disclosure of conflict of interest

None.

Address correspondence to: Xu-Sheng Liu and Zhi-Jun Pei, Department of Nuclear Medicine and Institute of Anesthesiology and Pain, Taihe Hospital, Hubei University of Medicine, Shiyan, Hubei, China. E-mail: lxsking@taihehospital.com (XSL); pzjzml1980@taihehospital.com (ZJP)

References

[1] Sung H, Ferlay J, Siegel RL, Laversanne M, Soerjomataram I, Jemal A and Bray F. Global cancer statistics 2020: GLOBOCAN estimates of incidence and mortality worldwide for 36 cancers in 185 countries. CA Cancer J Clin 2021; 71: 209-249.

[2] Thai AA, Solomon BJ, Sequist LV, Gainor JF and Heist RS. Lung cancer. Lancet 2021; 398: 535-554.

[3] Herbst RS, Morgensztern D and Boshoff C. The biology and management of non-small cell lung cancer. Nature 2018; 553: 446-454.

[4] Seguin L, Durandy M and Feral CC. Lung adenocarcinoma tumor origin: a guide for personalized medicine. Cancers (Basel) 2022; 14: 1759.

[5] Jiang Y, You J, Wu C, Kang Y, Chen F, Chen L and Wu W. High expression of DARS2 indicates poor prognosis in lung adenocarcinoma. J Clin Lab Anal 2022; 36: e24691.

[6] Jin X, Zhang H, Sui Q, Li M, Liang J, Hu Z, Cheng Y, Zheng Y, Chen Z, Lin M, Wang H and Zhan C. Identification and validation of the mitochondrial function related hub genes by unsupervised machine learning and multi-omics analyses in lung adenocarcinoma. Heliyon 2022; 8: e11966.

[7] Santarpia M, Aguilar A, Chaib I, Cardona AF, Fancelli S, Laguia F, Bracht JWP, Cao P, Molina-Vila MA, Karachaliou N and Rosell R. Non-small-cell lung cancer signaling pathways, metabolism, and PD-1/PD-L1 antibodies. Cancers (Basel) 2020; 12: 1475.

[8] Chi A, He X, Hou L, Nguyen NP, Zhu G, Cameron RB and Lee JM. Classification of non-small cell lung cancer's tumor immune micro-environment and strategies to augment its response to immune checkpoint blockade. Cancers (Basel) 2021; 13: 2924.

[9] Liu XS, Zhou LM, Yuan LL, Gao Y, Kui XY, Liu XY and Pei ZJ. NPM1 is a prognostic biomarker

involved in immune infiltration of lung adenocarcinoma and associated with m6A modification and glycolysis. Front Immunol 2021; 12: 724741.
[10] Teng PC, Liang Y, Yarmishyn AA, Hsiao YJ, Lin TY, Lin TW, Teng YC, Yang YP, Wang ML, Chien CS, Luo YH, Chen YM, Hsu PK, Chiou SH and Chien Y. RNA modifications and epigenetics in modulation of lung cancer and pulmonary diseases. Int J Mol Sci 2021; 22: 10592.
[11] Tsvetkov P, Coy S, Petrova B, Dreishpoon M, Verma A, Abdusamad M, Rossen J, Joesch-Cohen L, Humeidi R, Spangler RD, Eaton JK, Frenkel E, Kocak M, Corsello SM, Lutsenko S, Kanarek N, Santagata S and Golub TR. Copper induces cell death by targeting lipoylated TCA cycle proteins. Science 2022; 375: 1254-1261.
[12] Cobine PA and Brady DC. Cuproptosis: cellular and molecular mechanisms underlying copper-induced cell death. Mol Cell 2022; 82: 1786-1787.
[13] Shanbhag VC, Gudekar N, Jasmer K, Papageorgiou C, Singh K and Petris MJ. Copper metabolism as a unique vulnerability in cancer. Biochim Biophys Acta Mol Cell Res 2021; 1868: 118893.
[14] Jiang Y, Huo Z, Qi X, Zuo T and Wu Z. Copper-induced tumor cell death mechanisms and antitumor theragnostic applications of copper complexes. Nanomedicine (Lond) 2022; 17: 303-324.
[15] Li B, Severson E, Pignon JC, Zhao H, Li T, Novak J, Jiang P, Shen H, Aster JC, Rodig S, Signoretti S, Liu JS and Liu XS. Comprehensive analyses of tumor immunity: implications for cancer immunotherapy. Genome Biol 2016; 17: 174.
[16] Li T, Fan J, Wang B, Traugh N, Chen Q, Liu JS, Li B and Liu XS. TIMER: a web server for comprehensive analysis of tumor-infiltrating immune cells. Cancer Res 2017; 77: e108-e110.
[17] Li T, Fu J, Zeng Z, Cohen D, Li J, Chen Q, Li B and Liu XS. TIMER2.0 for analysis of tumor-infiltrating immune cells. Nucleic Acids Res 2020; 48: W509-W514.
[18] Tomczak K, Czerwińska P and Wiznerowicz M. The Cancer Genome Atlas (TCGA): an immeasurable source of knowledge. Contemp Oncol (Pozn) 2015; 19: A68-77.
[19] Barrett T, Wilhite SE, Ledoux P, Evangelista C, Kim IF, Tomashevsky M, Marshall KA, Phillippy KH, Sherman PM, Holko M, Yefanov A, Lee H, Zhang N, Robertson CL, Serova N, Davis S and Soboleva A. NCBI GEO: archive for functional genomics data sets--update. Nucleic Acids Res 2012; 41: D991-D995.
[20] Gao Y, Yuan L, Zeng J, Li F, Li X, Tan F, Liu X, Wan H, Kui X, Liu X, Ke C and Pei Z. eIF6 is potential diagnostic and prognostic biomarker that associated with 18F-FDG PET/CT features and immune signatures in esophageal carcinoma. J Transl Med 2022; 20: 303.
[21] Győrffy B. Survival analysis across the entire transcriptome identifies biomarkers with the highest prognostic power in breast cancer. Comput Struct Biotechnol J 2021; 19: 4101-4109.
[22] Mizuno H, Kitada K, Nakai K and Sarai A. PrognoScan: a new database for meta-analysis of the prognostic value of genes. BMC Med Genomics 2009; 2: 18.
[23] Gu Z, Gu L, Eils R, Schlesner M and Brors B. circlize implements and enhances circular visualization in R. Bioinformatics 2014; 30: 2811-2812.
[24] Yu G, Wang LG, Han Y and He QY. clusterProfiler: an R package for comparing biological themes among gene clusters. OMICS 2012; 16: 284-7.
[25] Li Y, Xiao J, Bai J, Tian Y, Qu Y, Chen X, Wang Q, Li X, Zhang Y and Xu J. Molecular characterization and clinical relevance of m(6)A regulators across 33 cancer types. Mol Cancer 2019; 18: 137.
[26] Sun N, Chu J, Hu W, Chen X, Yi N and Shen Y. A novel 14-gene signature for overall survival in lung adenocarcinoma based on the Bayesian hierarchical Cox proportional hazards model. Sci Rep 2022; 12: 27.
[27] Yang L, Zhang R, Guo G, Wang G, Wen Y, Lin Y, Zhang X, Yu X, Huang Z, Zhao D and Zhang L; written on behalf of the AME Thoracic Surgery Collaborative Group. Development and validation of a prediction model for lung adenocarcinoma based on RNA-binding protein. Ann Transl Med 2021; 9: 474.
[28] Zhang X, Dong W, Zhang J, Liu W, Yin J, Shi D and Ma W. A novel mitochondrial-related nuclear gene signature predicts overall survival of lung adenocarcinoma patients. Front Cell Dev Biol 2021; 9: 740487.
[29] Chen F, Wang Q and Zhou Y. The construction and validation of an RNA binding protein-related prognostic model for bladder cancer. BMC Cancer 2021; 21: 244.
[30] Guo C, Shao T, Jiang X, Wei D, Wang Z, Li M and Bao G. Comprehensive analysis of the functions and prognostic significance of RNA-binding proteins in bladder urothelial carcinoma. Am J Transl Res 2020; 12: 7160-7173.
[31] Wu Y, Liu Z, Wei X, Feng H, Hu B, Liu B, Luan Y, Ruan Y, Liu X, Liu Z, Wang S, Liu J and Wang T. Identification of the functions and prognostic values of RNA binding proteins in bladder cancer. Front Genet 2021; 12: 574196.
[32] Qin X, Li C, Guo T, Chen J, Wang HT, Wang YT, Xiao YS, Li J, Liu P, Liu ZS and Liu QY. Upregula-

tion of DARS2 by HBV promotes hepatocarcinogenesis through the miR-30e-5p/MAPK/NFAT5 pathway. J Exp Clin Cancer Res 2017; 36: 148.
[33] Zhan J, Sun S, Chen Y, Xu C, Chen Q, Li M, Pei Y and Li Q. MiR-3130-5p is an intermediate modulator of 2q33 and influences the invasiveness of lung adenocarcinoma by targeting NDUFS1. Cancer Med 2021; 10: 3700-3714.
[34] Yin J, Liu W, Li R, Liu J, Zhang Y, Tang W and Wang K. IARS2 silencing induces non-small cell lung cancer cells proliferation inhibition, cell cycle arrest and promotes cell apoptosis. Neoplasma 2016; 63: 64-71.
[35] Tian T, Ikeda J, Wang Y, Mamat S, Luo W, Aozasa K and Morii E. Role of leucine-rich pentatricopeptide repeat motif-containing protein (LRPPRC) for anti-apoptosis and tumourigenesis in cancers. Eur J Cancer 2012; 48: 2462-2473.
[36] Liu X, Xiang D, Xu C and Chai R. EIF3m promotes the malignant phenotype of lung adenocarcinoma by the up-regulation of oncogene CAPRIN1. Am J Cancer Res 2021; 11: 979-996.
[37] Germain C, Gnjatic S, Tamzalit F, Knockaert S, Remark R, Goc J, Lepelley A, Becht E, Katsahian S, Bizouard G, Validire P, Damotte D, Alifano M, Magdeleinat P, Cremer I, Teillaud JL, Fridman WH, Sautès-Fridman C and Dieu-Nosjean MC. Presence of B cells in tertiary lymphoid structures is associated with a protective immunity in patients with lung cancer. Am J Respir Crit Care Med 2014; 189: 832-844.
[38] Deng X, Su R, Weng H, Huang H, Li Z and Chen J. RNA N(6)-methyladenosine modification in cancers: current status and perspectives. Cell Res 2018; 28: 507-517.
[39] Muthusamy S. m(6)A mRNA methylation: a pleiotropic regulator of cancer. Gene 2020; 736: 144415.
[40] Yan M, Sun L, Li J, Yu H, Lin H, Yu T, Zhao F, Zhu M, Liu L, Geng Q, Kong H, Pan H and Yao M. RNA-binding protein KHSRP promotes tumor growth and metastasis in non-small cell lung cancer. J Exp Clin Cancer Res 2019; 38: 478.
[41] Huang Q, Guo H, Wang S, Ma Y, Chen H, Li H, Li J, Li X, Yang F, Qiu M, Zhao S and Wang J. A novel circular RNA, circXPO1, promotes lung adenocarcinoma progression by interacting with IGF2BP1. Cell Death Dis 2020; 11: 1031.
[42] Yan A, Song X, Liu B and Zhu K. IGF2BP3 worsens lung cancer through modifying long noncoding RNA CERS6-AS1/microRNA-1202 axis. Curr Med Chem 2023; 30: 878-891.
[43] Ma M, Wang W, Wang B, Yang Y, Huang Y, Zhao G and Ye L. The prognostic value of N6-methyladenosine RBM15 regulators in lung adenocarcinoma. Cell Mol Biol (Noisy-Le-Grand) 2022; 68: 130-139.
[44] Shi Y, Fan S, Wu M, Zuo Z, Li X, Jiang L, Shen Q, Xu P, Zeng L, Zhou Y, Huang Y, Yang Z, Zhou J, Gao J, Zhou H, Xu S, Ji H, Shi P, Wu DD, Yang C and Chen Y. YTHDF1 links hypoxia adaptation and non-small cell lung cancer progression. Nat Commun 2019; 10: 4892.
[45] Zhang X and Yang Q. Association between serum copper levels and lung cancer risk: a meta-analysis. J Int Med Res 2018; 46: 4863-4873.
[46] Chen Q, Wang Y, Yang L, Sun L, Wen Y, Huang Y, Gao K, Yang W, Bai F, Ling L, Zhou Z, Zhang X, Xiong J and Zhai R. PM2.5 promotes NSCLC carcinogenesis through translationally and transcriptionally activating DLAT-mediated glycolysis reprograming. J Exp Clin Cancer Res 2022; 41: 229.

Supplementary Table 1. Differential analysis results of Pan-cancer expression of DARS2

Tumor	Nor	p
BLCA.Tumor (n=408)	BLCA.Normal (n=19)	7.25E-08
BRCA.Tumor (n=1093)	BRCA.Normal (n=112)	2.81E-26
CESC.Tumor (n=304)	CESC.Normal (n=3)	3.30E-03
CHOL.Tumor (n=36)	CHOL.Normal (n=9)	5.98E-07
COAD.Tumor (n=457)	COAD.Normal (n=41)	6.15E-04
ESCA.Tumor (n=184)	ESCA.Normal (n=11)	3.00E-07
GBM.Tumor (n=153)	GBM.Normal (n=5)	3.00E-04
HNSC-HPV+.Tumor (n=97)	HNSC-HPV-.Tumor (n=421)	1.02E-04
HNSC.Tumor (n=520)	HNSC.Normal (n=44)	1.94E-16
KICH.Tumor (n=66)	KICH.Normal (n=25)	9.72E-06
KIRC.Tumor (n=533)	KIRC.Normal (n=72)	1.59E-29
KIRP.Tumor (n=290)	KIRP.Normal (n=32)	2.33E-04
LIHC.Tumor (n=371)	LIHC.Normal (n=50)	3.02E-20
LUAD.Tumor (n=515)	LUAD.Normal (n=59)	9.81E-27
LUSC.Tumor (n=501)	LUSC.Normal (n=51)	5.75E-27
PAAD.Tumor (n=178)	PAAD.Normal (n=4)	3.02E-01
PCPG.Tumor (n=179)	PCPG.Normal (n=3)	2.56E-02
PRAD.Tumor (n=497)	PRAD.Normal (n=52)	2.90E-04
READ.Tumor (n=166)	READ.Normal (n=10)	3.52E-02
SKCM.Tumor (n=103)	SKCM.Metastasis (n=368)	2.48E-07
STAD.Tumor (n=415)	STAD.Normal (n=35)	7.61E-18
THCA.Tumor (n=501)	THCA.Normal (n=59)	3.02E-08
UCEC.Tumor (n=545)	UCEC.Normal (n=35)	1.25E-13